

Bundle Adjustment in the Eager Mode

Zitong Zhan¹, Huan Xu², Zihang Fang³, Xinpeng Wei², Yaoyu Hu⁴, Chen Wang¹

Abstract—Bundle adjustment (BA) is a critical technique in various robotic applications, such as simultaneous localization and mapping (SLAM), augmented reality (AR), and photogrammetry. BA optimizes parameters such as camera poses and 3D landmarks to align them with observations. With the growing importance of deep learning in perception systems, there is an increasing need to integrate BA with deep learning frameworks for enhanced reliability and performance. However, widely-used C++-based BA frameworks, such as GTSAM, g²o, and Ceres, lack native integration with modern deep learning libraries like PyTorch. This limitation affects their flexibility, adaptability, ease of debugging, and overall implementation efficiency. To address this gap, we introduce an eager-mode BA framework seamlessly integrated with PyPose, providing PyTorch-compatible interfaces with high efficiency. Our approach includes GPU-accelerated, differentiable, and sparse operations designed for 2nd-order optimization, Lie group and Lie algebra operations, and linear solvers. Our eager-mode BA on GPU demonstrates substantial runtime efficiency, achieving an average speedup of 18.5×, 22×, and 23× compared to GTSAM, g²o, and Ceres, respectively. The source code will be made publicly available to benefit the entire community.

I. INTRODUCTION

Bundle adjustment (BA) is a fundamental technique in 3D vision, playing a crucial role in various applications such as virtual reality [1], photogrammetry [2], and simultaneous localization and mapping (SLAM) [3]. The primary goal of BA is to refine sensors' and environmental parameters, e.g., camera poses and 3D landmarks, so that the parameters are best fitted with observations, e.g., image pixel matching [4].

To enhance localization accuracy and preserve semantic information, integrating BA with data-driven methods has become a growing trend [3]–[7]. Achieving this often requires implementing BA within deep learning frameworks, such as PyTorch [8], which operates in the *eager mode*[†]. Remarkably, the *eager mode* execution has led to the success of PyTorch due to its various advantages such as ease of use and debugging, as well as the flexibility of Python syntax without sacrificing much of performance [9]. As a result, researchers have shown an overwhelming preference for eager mode programming [10]. Despite these strengths, no BA frameworks can function in the *eager mode* to match the flexibility and adaptability of deep learning frameworks, leading to several challenges and drawbacks.

Corresponding Email: {zitongz, chenw}@sairlab.org

¹Spatial AI & Robotics (SAIR) Lab, University at Buffalo, NY 14260

²Georgia Institute of Technology, GA 30332

³Northview High School, GA 30097

⁴Carnegie Mellon University, PA 15213

[†]*Eager mode* in machine learning frameworks such as PyTorch enables immediate execution of operations as they are called, allowing for dynamic computational graph construction and providing an intuitive, interactive development experience that simplifies debugging and experimentation.

Without eager mode, researchers are unable to build dynamic computational graphs for BA using Python syntax, which limits the flexibility of employing complex control flows, such as loops and conditionals. As a result, models cannot make data-dependent decisions during runtime, which is crucial for ensuring the robustness of BA, e.g., outlier rejection based on error pattern. This increases the difficulty of debugging and experimenting with prototypes. Additionally, optimizing BA separately from learning-based models could lead to model compounded errors, especially when the two components are optimized in different contexts [6].

Nevertheless, building BA frameworks in the *eager mode* is extremely challenging due to the involvement of a series of complicated algorithms, such as 2nd-order optimization [11], differentiation on Lie manifold [12], sparse Jacobian [13], and sparse linear algebra [14]. Moreover, designing flexible, modular, and extensible interfaces for all these operations in the eager mode is highly intricate and demands careful planning to ensure both adaptability and performance.

In this work, we present a new BA framework in the eager mode based on PyPose [15], our open-source library for robot learning. PyPose is fully compatible with PyTorch's eager mode and offers highly extensible interfaces for 2nd-order optimizations and differentiation on the Lie manifold. However, it currently lacks support for the sparse 2nd-order optimization. To solve this, we introduce AutoDiff and linear algebra operations for sparse problems in the eager mode, addressing sparse Jacobian of Lie group and 2nd-order optimization. Furthermore, we preserved the original interfaces, allowing users to easily take advantage of these new features by making minimal changes to their existing code. As a result, their extensibility is retained to the maximum extent, ensuring that users can easily adapt them for a broader scope.

Among them, computing a sparse Jacobian by AutoDiff is difficult in the eager mode. This is because PyTorch's autograd engine exhaustively computes every gradient in a dense Jacobian and cannot determine the existence of a gradient in advance. Therefore, the Jacobian sparsity pattern required for building the sparse matrix is unknown. To overcome this, we introduce a strategy that automatically traces data manipulation to determine the sparsity pattern.

Additionally, we leverage `LieTensor` in PyPose to represent the Lie group and Lie algebra for AutoDiff through the batched camera rotations. We reuse the native sparse `Tensor` in PyTorch to represent Jacobian, thus avoiding introducing self-defined data structures [16]. We implement new sparse linear solvers and basic math operations in the eager mode, ensuring the entire process of BA is efficient and highly parallelizable. In summary, our contributions include

- We present a new BA framework in the eager mode, showing that optimization traditionally requiring complex factor graphs can easily be carried out in Python. It seamlessly works with PyTorch and its autograd engine, allowing learning-based models to be easily combined.
- We introduce **sparsity-aware** AutoDiff for 2nd-order optimization, Lie groups and Lie algebras, and linear algebra, retaining original PyTorch interface design to extend their applicability to broader domains.
- The extensive experiments demonstrated the high efficiency of our BA framework on GPU, surpassing GTSAM by 18.5 \times , g²o by 22 \times , and Ceres by 23 \times in terms of runtime efficiency, even though our eager mode execution trades performance for flexibility.

II. RELATED WORK

A. Eager-mode Programming Interfaces

Eager mode [9] is an intuitive and user-friendly approach used in deep learning libraries to execute operations. It aligns closely with standard programming practices and interprets user commands during runtime. Debugging and interactive development become feasible because it provides immediate feedback in step-by-step execution. On the other hand, non-eager mode involves defining a computational graph first and then executing the graph as a whole. This approach can optimize performance during compile time, making it faster than eager mode but at the cost of usability.

PyTorch [9] is the first machine learning framework advocating eager mode usage, renowned for its flexible and intuitive programming style. It integrates seamlessly with the Python ecosystem and prioritizes simplicity and consistency. The eager mode design has made PyTorch a favorite among researchers and developers, leading even traditional non-eager mode frameworks to adopt similar programming models [17]. In terms of maintainability, it values simplicity in its internal implementation to allow for adaptability and rapid feature development in the fast-evolving AI field.

B. Factor Graph Non-linear Optimizers

GTSAM [16], g²o [18], and Ceres [14] are generalized non-eager mode non-linear optimizers capable of solving large scale problems with 2nd-order optimization. All of them offer high-accuracy solutions to BA problems. These libraries are designed for parallel CPU core usage but barely utilize the GPUs. DeepLM [19] attempts to build the Levenberg-Marquardt (LM) algorithm partially based on PyTorch. It relies on the autograd engine of PyTorch for calculating the Jacobian values, and implements the Jacobian product and the damped linear system using C++ and OpenMP [20] for parallelization on the CPU. Such an implementation choice makes it hard to maintain and is incompatible with the up-to-date PyTorch 2.0 [8]. To achieve end-to-end differentiability under an eager mode interface and for a simpler implementation, PyPose [21] provides a variety of non-linear solvers, including Gauss-Newton and LM, entirely in PyTorch. gradSLAM [22] is a SLAM demo project that includes an implementation of

differentiable Gauss-Newton using PyTorch. However, they ignored sparsity support [21], [22], making them impossible to be applied in even moderate-scale problems.

To the best of our knowledge, our BA framework provides the first exact eager mode 2nd-order optimizer compatible with PyTorch and utilizes sparse data structure for scalability.

C. Bundle Adjustment in Deep Learning

DROID-SLAM [5] is a deep learning-based SLAM system that performs recurrent iterative updates of camera pose and pixel-wise depth through a dense BA layer, enhancing accuracy and robustness. It uses the Gauss-Newton algorithm for simplicity and implements CUDA kernels from scratch specific to its use case. However, the solution is not generalizable to all settings nor easy to re-build. iMatching [4] is a self-supervised feature correspondence learning method that leverages BA as a supervisory signal to enhance the accuracy of feature matching and pose estimation. This approach allows feature-matching models to learn from arbitrary uninterrupted videos without requiring ground truth of camera pose or depth. Although based on PyTorch, its BA is implemented with GTSAM [16], limiting its extensibility.

III. PRELIMINARIES

To clarify the challenges of BA in eager mode, we first review non-linear least squares (NLS) optimization, using the Levenberg-Marquardt (LM) algorithm as an example.

A. Non-linear Least Squares

BA jointly refines camera parameters and 3D landmarks to minimize reprojection error between the observed 2D image points and the projected 3D points. In practice, BA is often formulated as a non-linear least squares (NLS) problem:

$$\theta^* = \arg \min_{\theta} \sum_{i=1}^C \sum_{j=1}^P \underbrace{\|\Pi(\zeta_i, \mathbf{p}_j, \mathbf{K}_i) - \mathbf{x}_{ij}\|_2^2}_{\mathbf{r}_{ij}}, \quad (1)$$

where Π represents the camera projection model, C is the number of camera poses, P is the number of 3D points, $\zeta_i \in \mathbb{SE}(3)$ is the i -th camera pose, \mathbf{K}_i is camera intrinsic parameters, $\mathbf{p}_j \in \mathbb{R}^3$ denotes 3D scene points, and \mathbf{x}_{ij} represents the observed 2D pixel location of the 3D point \mathbf{p}_j in the image of camera i . The goal of the optimization (1) is to refine parameters $\theta \doteq \{\zeta, \mathbf{p}\}$ to minimize the sum of squared reprojection errors \mathbf{r}_{ij} , thereby ensuring alignment between the 2D image observations and the 3D geometry. In this paper, we use quaternion to represent a rotation and denote all variables as vectors, thus camera poses $\zeta \in \mathbb{R}^{7C}$, 3D points $\mathbf{p} \in \mathbb{R}^{3P}$, and the residual $\mathbf{r} \in \mathbb{R}^{2PC}$.

B. Levenberg-Marquard Algorithm

The LM algorithm combines the Gauss-Newton and gradient descent methods to solve an NLS. The LM update rule iteratively adjusts the parameters θ (camera parameters ζ and 3D point locations \mathbf{p}) by solving a linear system:

$$(\mathbf{J}^T \mathbf{J} + \lambda \text{diag}(\mathbf{J}^T \mathbf{J})) \Delta \theta = -\mathbf{J}^T \mathbf{r}, \quad (2)$$

Algorithm 1 The Levenberg-Marquardt algorithm

Require: λ (damping), θ_0 (params)
for $t \leftarrow 1$ to T **do**
 $\mathbf{J} \leftarrow \frac{\partial \mathbf{r}_{\theta_{t-1}}}{\partial \theta_{t-1}}$
 $\mathbf{A} \leftarrow \mathbf{J}^\top \mathbf{J}$
 $\mathbf{A} \leftarrow \mathbf{A} + \lambda \cdot \text{diag}(\mathbf{A})$
 $\Delta \theta = \text{solver}(\mathbf{A}, -\mathbf{J}^\top \mathbf{r})$
 $\theta_t \leftarrow \theta_{t-1} + \Delta \theta$
end for
return θ_t

where \mathbf{r} is the vectorized reprojection residuals, $\mathbf{J} \doteq \frac{\partial \mathbf{r}}{\partial \theta} \in \mathbb{R}^{(2CP) \times (7C+3P)}$ is the Jacobian of the residuals with respect to the parameters, λ is a damping factor, and $\text{diag}(\mathbf{J}^\top \mathbf{J})$ is a diagonal matrix consisting of the diagonal elements of $\mathbf{J}^\top \mathbf{J}$. At each iteration, the parameters are updated as

$$\theta_t = \theta_{t-1} + \Delta \theta, \quad (3)$$

where the damping factor λ can either be fixed or adjusted based on whether the error is reduced, allowing the algorithm to balance between fast convergence and stability. A simplified version of the LM method is listed in Algorithm 1, whereas a fully implemented version can be found in [23].

IV. METHODOLOGY

Although the LM algorithm 1 is simple, the Jacobian matrix \mathbf{J} and the product $\mathbf{J}^\top \mathbf{J}$ in a BA problem are often large and have a sparse block structure. These characteristics often render a regular LM implementation [21] inadequate. These issues, including sparse Jacobian calculation and efficient sparse linear algebra in eager mode, will be addressed in Section IV-A and Section IV-B, respectively.

A. Sparse Jacobian

The Jacobian matrix \mathbf{J} in a BA problem is sparse due to the unique relationship between 3D landmarks and their 2D projections, i.e., reprojection residual on each 2D pixel \mathbf{r}_{ij} only depends on a single camera pose ζ_i and 3D landmarks \mathbf{p}_j , while all other parameters unrelated to the pixel have no gradients. As a result, tracking this sparsity pattern is crucial for efficient computation and optimization. However, PyTorch AutoDiff strategy is designed to handle general scenarios and computes every gradient, which is extremely inefficient[‡]. We next analyze the sparsity pattern and present an automatic sparsity tracking strategy for the eager mode.

1) *Sparsity Pattern and Representation:* Since all camera poses $\zeta \in \mathbb{R}^{7C}$, 3D points $\mathbf{p} \in \mathbb{R}^{3P}$, and the residuals $\mathbf{r} \in \mathbb{R}^{2PC}$ are vectorized variables, the Jacobian in BA is stored in a *sparse block* structure. A natural way is to partition the large matrix into smaller blocks to highlight the interactions

between vectors ζ_i , \mathbf{p}_j , and \mathbf{r}_{ij} [24]. Each block is a sub-Jacobian matrix, comprising the partial derivatives of the reprojection error with respect to a specific camera or point parameter. Therefore, each residual \mathbf{r}_{ij} is only associated with two blocks defined by $\mathbf{J}_{[\mathbf{r}_{ij}, \zeta_i]} \doteq \frac{\partial \mathbf{r}_{ij}}{\partial \zeta_i} \in \mathbb{R}^{2 \times 7}$ for camera poses and $\mathbf{J}_{[\mathbf{r}_{ij}, \mathbf{p}_j]} \doteq \frac{\partial \mathbf{r}_{ij}}{\partial \mathbf{p}_j} \in \mathbb{R}^{2 \times 3}$ for 3D points.

We represent the Jacobian tensors using the native `sparse_bsr` (Block Sparse Row) format [25], which is particularly designed for matrices with a block sparse structure. This retains the original form of Jacobian in matrix shape, and allows block $\mathbf{J}_{[\mathbf{r}_{ij}, \cdot]}$ to be directly indexed by the corresponding residual and parameter. Moreover, compared to other formats such as `sparse_coo` (Coordinate List) [26], it is more optimized for matrix-matrix operations such as $\mathbf{J}^\top \mathbf{J}$ frequently used in LM. Note that PyTorch lacks support for basic operations for `sparse_bsr` format, e.g., the matrix-matrix product, thus we implement all related operations in the eager mode so that the entire LM algorithm can be applied with standard Python operators. By only storing the sparse blocks, the space complexity can be reduced from $\mathcal{O}(n^2)$ to $\mathcal{O}(n)$, where $n = 7C + 3P$ is the number of parameters to optimize. This significant complexity reduction makes it practical for large-scale problems.

It is worth noting that previous BA frameworks such as GTSAM [16] employ a Jacobian *dictionary*, where each $\mathbf{J}_{[\mathbf{r}_{ij}, \cdot]}$ is stored with an identifier based on the input-output symbol $(\zeta_i | \mathbf{p}_j, \mathbf{r}_{ij})$. The existence of $\mathbf{J}_{[\mathbf{r}_{ij}, \cdot]}$ is determined by searching a factor graph, and the optimization process involves updating the Jacobian dictionary. However, this representation is unsuitable for eager mode frameworks, which lack the detailed symbol tracking required for graph searches. Also, the dictionary is a discrete data structure that is unfriendly for GPU parallelization. Consequently, the graph search becomes infeasible in the eager mode.

2) *Sparsity-aware AutoDiff in the Eager Mode:* PyTorch’s backward AutoDiff [27] streamlines gradient computation by eliminating the need for user intervention. During the backward pass, gradients are automatically calculated by traversing the computational graph in reverse and applying the chain rule [28]. We aim to achieve the same level of flexibility in graph traversal to efficiently compute sparse Jacobian matrices, which are crucial for many applications.

To ensure high efficiency and flexibility, the sparse block Jacobian is constructed by first calculating the Jacobian blocks $\mathbf{J}_{[\mathbf{r}_{ij}, \cdot]}$ and then placing them into their designated locations in the \mathbf{J} matrix. Although there’s an intuitive solution to traverse through each block and perform a backward pass one by one, it is inevitably slow. Instead, we compute all blocks within a single backpropagation pass and generate camera and point Jacobian blocks in batch, with stacked shapes of $\mathbb{R}^{(C \times P) \times 2 \times 7}$ and $\mathbb{R}^{(C \times P) \times 2 \times 3}$, respectively.

This requires us to trace the contribution of a parameter to all related residuals. Since each camera $\zeta_{(\cdot)}$ and point $\mathbf{p}_{(\cdot)}$ is re-used for in multiple pixel projections $\mathbf{x}_{(\cdot)}$, we replicate them in the forward pass to match each \mathbf{r}_{ij} with a unique copy of the required parameters (ζ_i, \mathbf{p}_j) . This

[‡]For example, the sample “Ladybug” in BAL dataset [13] with 1723 camera poses and 156k 3D points would produce a dense Jacobian consuming 2.6TB memory in double float precision and need 12 TFLOPs.

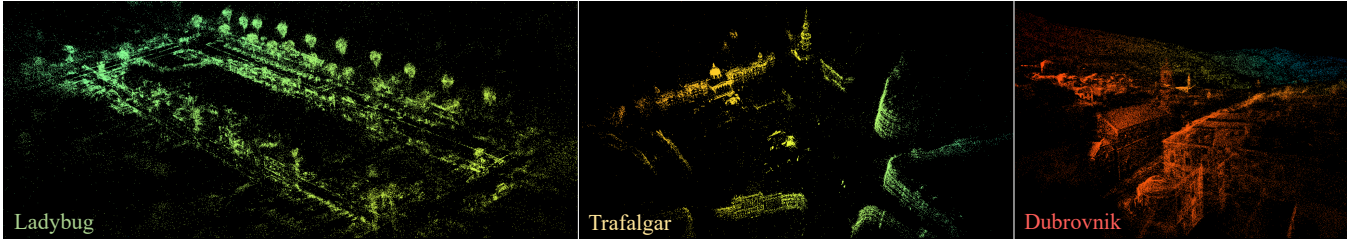


Fig. 1: **Qualitative results on the BAL dataset.** Our method successfully recovered the 3D geometry in the scene. Best viewed digitally.

allows calculating the camera projections \mathbf{x} in batch. More importantly, the unique copies of the parameters allow us to *simultaneously yet independently* backpropagate gradients from each residual \mathbf{r}_{ij} to ζ_i and \mathbf{p}_j , forming the blocks $\mathbf{J}_{[\mathbf{r}_{ij}, \zeta_i]}$ and $\mathbf{J}_{[\mathbf{r}_{ij}, \mathbf{p}_j]}$. In practice, we use the tensor indexing operation `tensor[indices]` to efficiently replicate batch samples, resulting in a contiguous data layout in memory [29]. This simple tensor usage is demonstrated in Section IV-C and is particularly effective on high-throughput GPU memory. In addition, we overload this operation so that it also records the indices for later use in the backward pass.

To backpropagate the Jacobian blocks in batch, we compose PyTorch functions `torch.func.jacrev` with `torch.func.vmap`. Specifically, we use `jacrev` to obtain the Jacobian block calculation for a single pixel residual. We then use `vmap` to apply this computation to the entire batch, generating all Jacobian blocks in parallel. The block locations are tracked from the applied indexing operations, where the sources of cameras and points are recorded. By having both the block locations and block values, we can recover the Jacobian in the `sparse_bsr` format.

B. Sparse Linear Algebra Operations

To complete the remaining steps of the LM algorithm, additional sparse linear algebra operations are necessary. However, PyTorch offers limited support for operations on sparse tensors. To overcome this limitation, we have developed a set of sparse linear operations that function in eager mode. Importantly, unlike libraries such as Ceres, g^2o , and GTSAM, which provide sparse operations tailored specifically to their proprietary data structure, our implementation is general-purpose and can be applied to any application, functioning like a standard Python operator.

1) *Matrix Multiplication:* Matrix multiplication plays a critical role in computing the Jacobian multiplication $\mathbf{J}^\top \mathbf{J}$, where \mathbf{J}^\top is a sparse matrix in Compressed Sparse Row (CSR) [30] or Block Sparse Row (BSR) format. The multiplication of two sparse matrices, commonly known as Sparse General Matrix-Matrix Multiplication (SpGEMM) [31], is essential for this computation. We implement the CSR multiplication using the cuSPARSE library [32], leveraging its optimized routines for sparse linear algebra operations. For the BSR format, we develop custom CUDA kernels to handle the block-structured sparsity efficiently.

These sparse matrix operations are registered to the PyTorch operator dispatcher. Users can perform matrix multiplication using the PyTorch syntax `mat1 @ mat2` with

previously unsupported sparse types. This design choice ensures that no modifications to the native eager mode API or user code are necessary, preserving the ease of use while providing advanced sparse linear algebra capabilities.

2) *Matrix-Vector Product:* The matrix-vector product is for computing $\mathbf{J}^\top \mathbf{r}$, where \mathbf{J}^\top is sparse while \mathbf{r} is a dense vector. This operation, commonly referred to as Sparse Matrix-Vector product (SpMV) [33], is one of the few sparse operations natively supported by PyTorch, which internally utilizes the cuSPARSE library for efficient computation.

3) *Diagonal Clamping and Scaling:* Diagonal clamping and scaling are essential operations in various numerical algorithms, especially when adjusting the diagonal elements of a matrix for stability or regularization purposes. These operations are represented by functions such as `diagonal_clamp(min, max)`, which clamps the diagonal elements within a specified range to ensure numerical stability, and `$\lambda \cdot \text{diag}(\mathbf{A})$` , which scales the diagonal elements of matrix \mathbf{A} by a factor λ . Since PyTorch lacks native supports for these operations with sparse matrices, we implemented them using custom Triton kernels [34]. This allows diagonal clamping and scaling directly on sparse matrices.

4) *Sparse Linear Solvers:* Sparse linear solvers play a crucial role in computing parameter updates within the LM algorithm. The task involves solving a linear system of the form $\mathbf{A}\mathbf{x} = \mathbf{b}$, which is commonly expressed in code as `$\mathbf{x} = \text{solver}(\mathbf{A}, \mathbf{b})$` . In the context of LM, the matrix $\mathbf{A} = \mathbf{J}^\top \mathbf{J} + \lambda \text{diag}(\mathbf{J}^\top \mathbf{J})$ is a sparse symmetric positive-definite (SPD) matrix, and the vector $\mathbf{b} = -\mathbf{J}^\top \mathbf{r}$ is dense. The goal in each iteration is to find the update $\Delta\theta$ by solving the linear system $\mathbf{A}\Delta\theta = \mathbf{b}$, as required by (2).

Linear solvers are generally classified into direct and iterative methods. Direct solvers, such as those utilizing Cholesky [35] or LU decomposition [36] with pivoting, exploit the properties of SPD matrices to compute exact solutions in a finite number of steps. These methods are highly efficient for small to medium-sized problems. Iterative solvers, like the preconditioned conjugate gradient (PCG) method [37], approximate the solution through successive iterations, which can be more efficient and scalable for large, sparse systems.

To address varying problem scales, we provide two solver implementations: (1) **Sparse Cholesky Solver:** Designed for small-scale systems, this solver leverages the Cholesky decomposition to compute exact solutions efficiently; and (2) **Sparse Preconditioned Conjugate Gradient (PCG) Solver:** Suited for large-scale SPD systems, our PCG solver incorporates the preconditioning strategy from [13] to en-

hance numerical stability and accelerate convergence.

Our implementation focuses on concise sparse operators and maintains compatibility with the existing PyPose API for dense linear solvers [38]. This design choice ensures that our optimizer is easy to deploy in research settings and can be readily extended to accommodate more complex nonlinear optimization strategies. By fully exploiting GPU throughput, our approach enables the LM algorithm to be seamlessly executed in the eager execution mode, allowing for straightforward and efficient code development.

C. Minimum Runnable Code for BA in the Eager Mode

Due to the minimal API changes, the users can re-use the same code style of dense LM provided by PyPose [21] for our new sparse LM. A minimum runnable code example for BA in the eager mode with 1 camera and 8 points is listed below. To automatically balance the convergence rate and stability, a trust region strategy `TrustRegion` [39] can be applied to dynamically adjust the damping factor λ .

```
import torch, pypose as pp
from torch import nn, tensor
from pypose.optim import LM
from pypose.optim.strategy import TrustRegion
from pypose.optim.scheduler import StopOnPlateau

class Residual(nn.Module):
    def __init__(self, cameras, points):
        super().__init__()
        cameras = pp.SE3(cameras)
        self.poses = nn.Parameter(cameras)
        self.points = nn.Parameter(points)

    def forward(self, observes, K, cidx, pidx):
        poses = self.poses[cidx]
        points = self.points[pidx]
        projs = pp.point2pixel(point, poses, K)
        return projs - observes

torch.set_default_device("cuda")
C, P, fx, fy, cx, cy = 1, 8, 200, 200, 100, 100
K = tensor([[fx, 0, cx], [0, fy, cy], [0, 0, 1]])
cameras = pp.randn_SE3(C)
points = torch.randn(P, 3)
observes = torch.randn(P, 2)
cidx = torch.zeros(P, dtype=torch.int32)
pidx = torch.arange(P, dtype=torch.int32)
input = (observes, K, cidx, pidx)

model = Residual(cameras, points)
strategy = TrustRegion(damping=1e-6)
optimizer = LM(model, strategy=strategy)
scheduler = StopOnPlateau(optimizer, steps=10)

while scheduler.continual():
    loss = optimizer.step(input)
    scheduler.step(loss)
```

V. EXPERIMENTS

We next conduct extensive experiments to compare our BA in the eager mode with the popular BA frameworks.

A. Datasets, Baseline, Platforms, and Metrics

We conduct experiments on BA using BAL [13] and 1DSfM [40] datasets. The BAL dataset provides the initial estimations of 3D maps and camera locations. While 1DSfM

only provides raw images of the wild on Internet photo collections. Following [19], we generate the initial map using COLMAP with its bundle adjustment disabled.

We will conduct experiments using our PCG and Cholesky sparse linear solvers, which will be denoted as Ours (PCG) and Ours (Cholesky). They will be compared against the most widely-used BA frameworks, including Ceres [14], g^2o [18], and GTSAM [16]. Ceres is widely regarded as the leading BA library, known for its robustness and scalability to efficiently leverage a large number of CPU cores. Additionally, to ensure their best efficiency on CPU, we compiled GTSAM with Intel OneTBB [41], and g^2o and Ceres were built using OpenMP [20], with an optimization flag “-O3” applied. All the experiments were conducted on dual-socket CPUs with 64 physical cores and 512 GB of memory. We will also compare with the GPU-based framework DeepLM [19]. The performance will be presented using an Nvidia RTX 4090 GPU with double-precision floating point.

For evaluation, we assess the frameworks based on two metrics: mean squared error (MSE) in pixels to measure accuracy, and runtime in seconds to evaluate efficiency. These metrics allow for a comprehensive comparison of the quality and performance of the different BA methods.

B. Overall Performance

1) *BAL Dataset*: The performance comparison on the BAL dataset is presented in Table I. Our BA in the eager mode archives much higher efficiency, i.e., 4.4 \times , 6.65 \times , and 16 \times faster than GTSAM, g^2o , and Ceres, respectively. It is observed that all the BA frameworks except GTSAM can converge here, their precision in terms of MAE is comparable. We also noticed that Ours (Cholesky) achieves higher efficiency than Ours (PCG) in the scenes of “Trafalgar” and “Dubrovnik”. This is because “Trafalgar” has less number of parameters and “Dubrovnik” has an ill-posed linear system for PCG to solve. The qualitative results are shown in Fig. 1, where a high level of detail is reconstructed.

2) *1DSfM Dataset*: We present the overall performance on the 1DSfM dataset in Table II, where all frameworks share a similar final error. In terms of runtime efficiency, our BA framework surpasses GTSAM by 36 \times , g^2o by 43 \times , and Ceres by 40 \times in running speed, further demonstrating a consistently high efficiency of our BA in the eager mode.

3) *Scalability*: We next demonstrate the scalability of our BA in terms of the number of optimizable parameters. Fig. 2 illustrates the runtime speedup of our PCG optimizer relative to g^2o , GTSAM, and Ceres on the 1DSfM data samples. The plot reveals a general trend: as the problem scale increases, our BA demonstrates **exponentially** increased efficiency, reaching up to 136 \times , 166 \times , and 163 \times higher efficiency compared to g^2o , GTSAM, and Ceres, respectively. On small samples, our performance is bounded by the efficiency of the Python interpreter and thus is similar to other libraries. Despite eager mode’s performance limitations without compile-time optimization, the significant speedups result from our sparsity-aware algorithm, which efficiently leverages inherent sparsity and enables effective GPU parallelism.

TABLE I: Performance comparison with CPU-based BA frameworks on the BAL dataset.

Scene	Camera	Points	Pixels	GTSAM [16]		g ² o [18]		Ceres [14]		Ours (PCG)		Ours (Cholesky)	
				Time↓	Error↓	Time↓	Error↓	Time↓	Error↓	Time↓	Error↓	Time↓	Error↓
Ladybug	1723	156502	678718	12.43	2.540	59.12	1.313	177.15	1.146	1.60	1.120	6.01	1.134
Trafalgar	257	65132	225811	8.47	0.896	7.25	0.863	13.41	0.856	5.81	0.854	1.27	0.853
Dubrovnik	356	226730	1255268	41.80	0.787	28.18	0.789	36.71	0.787	32.10	0.793	6.93	0.791
Overall				62.70	1.408	94.55	0.988	227.27	0.92	39.51	0.922	14.21	0.926

TABLE II: Performance comparison with CPU-based BA frameworks on the IDSfM dataset.

Scene	Camera	Points	Pixels	GTSAM [16]		g ² o [18]		Ceres [14]		Ours (PCG)		Ours (Cholesky)	
				Time↓	Error↓	Time↓	Error↓	Time↓	Error↓	Time↓	Error↓	Time↓	Error↓
Union Square	166	3643	39651	9.53	2.365	0.78	2.617	2.15	2.324	1.21	2.358	0.33	2.377
P. del Popolo	317	13294	71055	10.79	3.104	5.64	3.104	8.42	3.102	1.61	2.925	1.16	2.928
Ellis Island	287	17565	64697	8.48	3.473	3.68	3.502	9.28	3.446	1.07	3.449	0.60	3.478
NYC Library	265	11247	50103	5.38	2.857	4.50	2.857	2.39	2.855	1.14	2.856	0.53	2.855
M. N. Dame	475	28209	147250	22.82	3.498	16.97	3.444	18.41	3.426	1.30	3.427	1.25	3.426
Gen. markt	745	32940	128472	10.82	4.793	45.45	2.968	30.66	2.922	1.62	2.925	1.16	2.928
Alamo	741	82801	536967	64.73	3.728	32.57	3.817	63.14	3.726	3.25	3.727	3.59	3.727
Yorkminster	64	3432	16351	2.70	2.244	0.19	2.323	1.67	2.059	2.43	2.090	0.59	2.094
Roman Forum	905	44245	151704	15.56	3.128	53.20	2.988	34.45	2.982	2.19	2.980	0.97	2.983
V. Cathedral	712	35688	170443	39.06	2.652	55.61	2.667	54.45	2.634	1.90	2.636	2.20	2.636
M. Metropolis	97	4981	21930	2.38	2.612	0.49	2.591	1.50	2.588	0.86	2.598	0.29	2.593
Piccadilly	1898	83234	363139	233.57	3.737	454.24	3.484	290.14	3.419	2.53	3.418	13.71	3.423
T. of London	327	13156	58179	9.45	2.303	5.67	2.245	13.87	2.098	1.28	2.108	0.77	2.108
Trafalgar	4159	130027	572171	494.02	3.387	405.56	3.342	486.15	3.311	2.96	3.241	12.40	3.307
Overall				929.28	3.134	1084.55	2.996	1016.67	2.921	25.35	2.910	39.55	2.919

TABLE III: Comparison with GPU-based method DeepLM.

Scene	DeepLM [19]		Ours (Best)	
	Time↓	Error↓	Time↓	Error↓
Ladybug	5.87	1.121	1.60	1.120
Trafalgar	3.44	0.858	1.27	0.853
Dubrovnik	13.10	0.787	6.93	0.791
BAL Overall	22.41	0.922	9.80	0.921
Union Square	1.31	2.330	0.33	2.377
P. del Popolo	1.45	3.103	1.16	2.928
Ellis Island	1.46	3.448	0.60	3.478
NYC Library	1.40	2.855	0.53	2.855
M. N. Dame	1.76	3.426	1.25	3.426
Gen. markt	1.77	2.926	1.16	2.928
Alamo	3.43	3.727	3.25	3.727
Yorkminster	1.24	2.089	0.59	2.094
Roman Forum	1.65	2.984	0.97	2.983
V. Cathedral	2.04	2.636	1.90	2.636
M. Metropolis	1.20	2.589	0.29	2.593
Piccadilly	2.28	3.419	2.53	3.418
T. of London	1.42	2.103	0.77	2.108
Trafalgar	3.05	3.241	2.96	3.241
IDSfM Overall	25.45	2.92	18.29	2.913

4) *Comparison with GPU-based framework:* As shown in Table III, our BA framework achieves both better precision and higher efficiency than DeepLM [19], the state-of-the-art PyTorch-based BA framework. Specifically, we require 56% and 28% less runtime than DeepLM on the BAL and IDSfM datasets, respectively. Note that although DeepLM is based on PyTorch, it does not support eager mode and

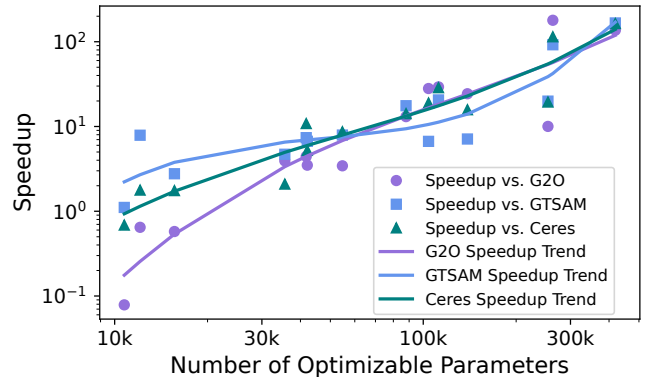


Fig. 2: Speedup of our BA relative to other frameworks exponentially increases with the number of optimizable parameters.

lacks extensibility to other applications since its sparsity is addressed by a non-native data structure.

VI. CONCLUSIONS & DISCUSSIONS

We presented a highly extensible and scalable eager-mode BA framework, which can seamlessly integrate with modern deep learning frameworks. By leveraging GPU acceleration, differentiable operations, and sparse linear operations, our new BA framework offers up to hundreds of times speed-up than widely-used CPU-based BA frameworks. Nevertheless, our current implementation is not optimized for computation on CPUs. Additionally, since memory allocation and release are managed by Python’s automatic garbage collection mechanism, our BA framework may have a higher memory consumption than the C++-based frameworks.

REFERENCES

- [1] Y. Jiang, C. Yu, T. Xie, X. Li, Y. Feng, H. Wang, M. Li, H. Lau, F. Gao, Y. Yang, and C. Jiang, "VR-GS: A physical dynamics-aware interactive gaussian splatting system in virtual reality," *arXiv preprint arXiv:2401.16663*, 2024.
- [2] X. He, J. Sun, Y. Wang, S. Peng, Q. Huang, H. Bao, and X. Zhou, "Detector-free structure from motion," *CVPR*, 2024.
- [3] K. Xu, Y. Hao, S. Yuan, C. Wang, and L. Xie, "AirVO: An illumination-robust point-line visual odometry," in *IEEE/RSJ International Conference on Intelligent Robots and Systems (IROS)*, 2023. [Online]. Available: <https://arxiv.org/pdf/2212.07595.pdf>
- [4] Z. Zhan, D. Gao, Y.-J. Lin, Y. Xia, and C. Wang, "iMatching: Imperative correspondence learning," in *European Conference on Computer Vision (ECCV)*, 2024. [Online]. Available: <https://arxiv.org/pdf/2312.02141.pdf>
- [5] Z. Teed and J. Deng, "Droid-slam: Deep visual slam for monocular, stereo, and rgb-d cameras," *Advances in Neural Information Processing Systems*, vol. 34, pp. 16 558–16 569, 2021.
- [6] C. Wang, K. Ji, J. Geng, Z. Ren, T. Fu, F. Yang, Y. Guo, H. He, X. Chen, Z. Zhan, Q. Du, S. Su, B. Li, Y. Qiu, Y. Du, Q. Li, Y. Yang, X. Lin, and Z. Zhao, "Imperative learning: A self-supervised neural-symbolic learning framework for robot autonomy," *arXiv preprint arXiv:2406.16087*, 2024. [Online]. Available: <https://arxiv.org/abs/2406.16087>
- [7] T. Fu, S. Su, Y. Lu, and C. Wang, "iSLAM: Imperative SLAM," *IEEE Robotics and Automation Letters (RA-L)*, 2024. [Online]. Available: <https://arxiv.org/pdf/2306.07894.pdf>
- [8] J. Ansel, E. Yang, H. He, N. Gimelshein, A. Jain, M. Voznesensky, B. Bao, P. Bell, D. Berard, E. Burovski, G. Chauhan, A. Chourdia, W. Constable, A. Desmaison, Z. DeVito, E. Ellison, W. Feng, J. Gong, M. Gschwind, B. Hirsh, S. Huang, K. Kalambarkar, L. Kirsch, M. Lazos, M. Lezcano, Y. Liang, J. Liang, Y. Lu, C. K. Luk, B. Maher, Y. Pan, C. Puhrsch, M. Reso, M. Saroufim, M. Y. Siraiichi, H. Suk, S. Zhang, M. Suo, P. Tillet, X. Zhao, E. Wang, K. Zhou, R. Zou, X. Wang, A. Mathews, W. Wen, G. Chanan, P. Wu, and S. Chintala, "PyTorch 2: Faster machine learning through dynamic python bytecode transformation and graph compilation," in *Proceedings of the 29th ACM International Conference on Architectural Support for Programming Languages and Operating Systems, Volume 2*, ser. ASPLOS '24. New York, NY, USA: Association for Computing Machinery, 2024, p. 929–947. [Online]. Available: <https://doi.org/10.1145/3620665.3640366>
- [9] A. Paszke, S. Gross, F. Massa, A. Lerer, J. Bradbury, G. Chanan, T. Killeen, Z. Lin, N. Gimelshein, L. Antiga, A. Desmaison, A. Kopf, E. Yang, Z. DeVito, M. Raison, A. Tejani, S. Chilamkurthy, B. Steiner, L. Fang, J. Bai, and S. Chintala, "PyTorch: An Imperative Style, High-Performance Deep Learning Library," in *Advances in Neural Information Processing Systems 32*, H. Wallach, H. Larochelle, A. Beygelzimer, F. d'Alché Buc, E. Fox, and R. Garnett, Eds. Curran Associates, Inc., 2019, pp. 8024–8035.
- [10] H. He, "The state of machine learning frameworks in 2019," *The Gradient*, 2019.
- [11] C. Zach, "Robust bundle adjustment revisited," in *Computer Vision – ECCV 2014*, D. Fleet, T. Pajdla, B. Schiele, and T. Tuytelaars, Eds. Cham: Springer International Publishing, 2014, pp. 772–787.
- [12] J. Solà, J. Deray, and D. Atchuthan, "A micro lie theory for state estimation in robotics," 2021. [Online]. Available: <https://arxiv.org/abs/1812.01537>
- [13] S. Agarwal, N. Snavely, S. M. Seitz, and R. Szeliski, "Bundle adjustment in the large," in *European Conference on Computer Vision (ECCV)*. Springer, 2010, pp. 29–42.
- [14] S. Agarwal, K. Mierle, and The Ceres Solver Team, "Ceres Solver," Oct. 2023. [Online]. Available: <https://github.com/ceres-solver/ceres-solver>
- [15] Z. Zhan, X. Li, Q. Li, H. He, A. Pandey, H. Xiao, Y. Xu, X. Chen, K. Xu, K. Cao, Z. Zhao, Z. Wang, H. Xu, Z. Fang, Y. Chen, W. Wang, X. Fang, Y. Du, T. Wu, X. Lin, Y. Qiu, F. Yang, J. Shi, S. Su, Y. Lu, T. Fu, K. Dantu, J. Wu, L. Xie, M. Hutter, L. Carlone, S. Scherer, D. Huang, Y. Hu, J. Geng, and C. Wang, "PyPose v0.6: The imperative programming interface for robotics," in *IEEE/RSJ International Conference on Intelligent Robots and Systems (IROS) Workshop*, 2023. [Online]. Available: <https://arxiv.org/abs/2309.13035>
- [16] F. Dellaert and Contributors, "borglab/gtsam," May 2022. [Online]. Available: <https://github.com/borglab/gtsam>
- [17] A. Agrawal, A. N. Modi, A. Passos, A. Lavoie, A. Agarwal, A. Shankar, I. Ganichev, J. Levenberg, M. Hong, R. Monga, and S. Cai, "Tensorflow eager: A multi-stage, python-embedded dsl for machine learning," 2019. [Online]. Available: <https://arxiv.org/abs/1903.01855>
- [18] R. Kümmerle, G. Grisetti, H. Strasdat, K. Konolige, and W. Burgard, "G2o: A general framework for graph optimization," in *IEEE Int. Conf. on Robotics and Automation (ICRA)*, 06 2011, pp. 3607 – 3613.
- [19] J. Huang, S. Huang, and M. Sun, "DeepIm: Large-scale nonlinear least squares on deep learning frameworks using stochastic domain decomposition," in *Proceedings of the IEEE Conference on Computer Vision and Pattern Recognition*, 2021, pp. 10 308–10 317.
- [20] OpenMP Architecture Review Board, "OpenMP application program interface version 3.0," May 2008. [Online]. Available: <http://www.openmp.org/mp-documents/spec30.pdf>
- [21] C. Wang, D. Gao, K. Xu, J. Geng, Y. Hu, Y. Qiu, B. Li, F. Yang, B. Moon, A. Pandey, Aryan, J. Xu, T. Wu, H. He, D. Huang, Z. Ren, S. Zhao, T. Fu, P. Reddy, X. Lin, W. Wang, J. Shi, R. Talak, K. Cao, Y. Du, H. Wang, H. Yu, S. Wang, S. Chen, A. Kashyap, R. Bandaru, K. Dantu, J. Wu, L. Xie, L. Carlone, M. Hutter, and S. Scherer, "PyPose: A library for robot learning with physics-based optimization," in *IEEE/CVF Conference on Computer Vision and Pattern Recognition (CVPR)*, 2023. [Online]. Available: <https://arxiv.org/pdf/2209.15428.pdf>
- [22] K. M. Jatavallabhula, G. Iyer, and L. Paull, "∇slam: Dense slam meets automatic differentiation," in *2020 IEEE International Conference on Robotics and Automation (ICRA)*. IEEE, 2020, pp. 2130–2137.
- [23] "pypose.optim.levenbergmarquardt," <https://pypose.org/docs/main/generated/pypose.optim.LevenbergMarquardt/>.
- [24] M. Zheng, N. Chen, J. Zhu, X. Zeng, H. Qiu, Y. Jiang, X. Lu, and H. Qu, "Distributed bundle adjustment with block-based sparse matrix compression for super large scale datasets," in *IEEE/CVF International Conference on Computer Vision (ICCV)*, 2023. [Online]. Available: <https://arxiv.org/abs/2307.08383>
- [25] "PyTorch sparse bsr tensor documentation," <https://pytorch.org/docs/stable/sparse.html#sparse-bsr-tensor>, 2024.
- [26] "Sparse Matrix - Coordinate List (COO)," [https://en.wikipedia.org/wiki/Sparse_matrix#Coordinate_list_\(COO\)](https://en.wikipedia.org/wiki/Sparse_matrix#Coordinate_list_(COO)), 2024, accessed: 2024-09-12.
- [27] "Automatic differentiation with torch.autograd," https://pytorch.org/tutorials/beginner/basics/autogradqs_tutorial.html.
- [28] "Automatic Differentiation," 2024, [Online]; accessed 12-September-2024. [Online]. Available: https://en.wikipedia.org/wiki/Automatic_differentiation#Forward_and_reverse_accumulation
- [29] "Tensor Indexing API," https://pytorch.org/cppdocs/notes/tensor_indexing.html, 2024, accessed: 2024-09-13.
- [30] "PyTorch Sparse CSR Tensor documentation," <https://pytorch.org/docs/stable/sparse.html#sparse-csr-tensor>, 2024.
- [31] F. G. Gustavson, "Two fast algorithms for sparse matrices: Multiplication and permuted transposition," *ACM Trans. Math. Softw.*, vol. 4, no. 3, p. 250–269, sep 1978. [Online]. Available: <https://doi.org/10.1145/355791.355796>
- [32] NVIDIA Corporation, "cusparse library," <https://docs.nvidia.com/cuda/cusparse/index.html>, 2024, accessed: 2024-09-13.
- [33] J. H. Wilkinson and C. B. Moler, *Matrix computations*. GBR: John Wiley and Sons Ltd., 2003, p. 1103–1109.
- [34] Triton Contributors, "Triton language and compiler," <https://github.com/triton-lang/triton>, 2024, accessed: 2024-09-13.
- [35] "Note sur une méthode de résolution des équations normales provenant de l'application de la méthode des moindres carrés a un système d'équations linéaires en nombre inférieur a celui des inconnues. — application de la méthode a la résolution d'un système défini d'équations linéaires," *Bulletin géodésique*, vol. 2, no. 1, pp. 67–77, 1924. [Online]. Available: <https://doi.org/10.1007/BF03031308>
- [36] A. Schwarzenberg-Czerny, "On matrix factorization and efficient least squares solution," *aaps*, vol. 110, p. 405, Apr. 1995.
- [37] P. Concus, G. Golub, and G. Meurant, "Block preconditioning for the conjugate gradient method," no. LBL-14856, 1982. [Online]. Available: <https://escholarship.org/uc/item/0j60b61v>
- [38] "PyPose linear solver," <https://pypose.org/docs/main/generated/pypose.optim.solver.PIN/>.
- [39] D. C. Sorensen, "Newton's method with a model trust-region modification," University of North Texas Libraries, UNT Digital Library, Tech. Rep., September 1980, accessed: September 13, 2024. [Online]. Available: <https://digital.library.unt.edu/ark:/67531/metadec283479/>

- [40] K. Wilson and N. Snavely, "Robust global translations with 1dsfm," in *Proceedings of the European Conference on Computer Vision (ECCV)*, 2014.
- [41] Intel Corporation, "oneapi threading building blocks (onetbb)," <https://www.intel.com/content/www/us/en/developer/tools/oneapi/onetbb.html>, 2021, version 2021.5.